Endocrine, vol. 7, no. 1, 15–32, August 1997 0969-711X/97/7:15-32/$12.50

Carbohydrate and Peptide Structure of the α- and β-Subunits of Human Chorionic Gonadotropin from Normal and Aberrant Pregnancy and Choriocarcinoma

Margaret M. Elliott,[1] Andrew Kardana,[1] Joyce W. Lustbader,[2] and Laurence A. Cole[1]

[1]Department of Obstetrics and Gynecology, Yale University School of Medicine, New Haven, CT; and [2]Department of Obstetrics and Gynecology, Center for Reproductive Sciences, Columbia University, New York, NY

Human chorionic gonadotropin (hCG), purified from the urine of 14 individuals with normal pregnancy, diabetic pregnancy, hydatidiform mole, or choriocarcinoma, plus two hCG standard preparations, was examined for concurrent peptide-sequence and asparagine (N)- and serine (O)-linked carbohydrate heterogeneity. Protein-sequence analysis was used to measure amino-terminal heterogeneity and the "nicking" of internal peptide bonds. The use of high-pH anion-exchange chromatography coupled with the increased sensitivity of pulsed amperometric detection (HPAE/PAD) revealed that distinct proportions of both hCG α- and β-subunits from normal and aberrant pregnancy are hyperglycosylated, and that it is the extent of the specific subunit hyperglycosylation that significantly increases in malignant disease.

Peptide-bond nicking was restricted to a single linkage (β47-48) in normal and diabetic pregnancy, but occurred at two sites in standard preparations, at three sites in hydatidiform mole, and at three sites in choriocarcinoma β-subunit. In the carbohydrate moiety, α-subunit from normal pregnancy hCG contained nonfucosylated, mono- and biantennary N-linked structures (49.3 and 36.7%, means); fucosylated biantennary and triantennary oligosaccharides were also identified (7.3 and 6.9%). In choriocarcinoma α-subunit, the level of fucosylated biantennary increased, offset by a parallel decrease in the predominant biantennary structure of normal pregnancy ($P < 0.0001$). The β-subunit from normal pregnancy hCG contained fucosylated and nonfucosylated biantennary N-linked structures; however, mono- and triantennary oligosaccharides were also identified (4.6 and 13.7%). For O-linked glycans, in β-subunit from normal pregnancy, disaccharide-core structure predominated, whereas tetrasaccharide-core structure was also detected (15.6%). A trend was demonstrated in β-subunit: the proportions of the nonpredominating N- and O-linked oligosaccharides increased stepwise from normal pregnancy to hydatidiform mole to choriocarcinoma. The increases were: for monoantennary oligosaccharide, 4.6 to 6.8 to 11.2%; for triantennary, 13.7 to 26.7 to 51.5% and, for O-linked tetrasaccharide-core structure, 15.6 to 23.0 to 74.8%. For hCG from individual diabetic pregnancy, the principal N-linked structure (34.7%) was consistent with a biantennary oligosaccharide previously reported only in carcinoma; and sialylation of both N- and O-linked antennae was significantly decreased compared to that of normal pregnancy.

Taken collectively, the distinctive patterns of subunit-specific, predominant oligosaccharides appear to reflect the steric effect of local protein structure during glycosylation processes. The evidence of alternative or "hyperbranched" glycoforms on both α- and β-subunits, seen at low levels in normal pregnancy and at increased or even predominant levels in malignant disease, suggests alternative substrate accessibility for Golgi processing enzymes, α1,6fucosyltransferase and *N*-acetylglucosaminyltransferase IV, in distinct proportions of subunit molecules.

Key Words: HCG α- and β-subunits; aberrant pregnancy; diabetic pregnancy; carcinoma; N- and O-linked glycans.

Introduction

Human chorionic gonadotropin (hCG), a glycoprotein hormone, is produced by normal trophoblast cells of the placenta during pregnancy, by hyperplastic cells in hydatidiform mole and malignant cells in choriocarcinoma, and by testicular and other, nontrophoblastic neoplasms. The binding of hCG to plasma membrane receptors in the ovary and testis activates the adenylate cyclase enzyme system,

Received March 17, 1997; Accepted May 7, 1997

Author to whom all correspondence and reprint requests should be addressed: Margaret M. Elliott, Department of Molecular Biophysics and Biochemistry, Yale University School of Medicine, 333 Cedar St., New Haven, CT 06510.

α-subunit, molecular weight: 10,207 (peptide) + 3,756 (carbohydrate)

ala-pro-asp-val-gln-asp-cys-pro-glu-cys-thr-leu-gln-glu-asp-pro-phe-phe-ser-gln-pro-gly-ala-pro-ile-leu-
1 2↑3↑4 N
gln-cys-met-gly-cys-cys-phe-ser-arg-ala-tyr-pro-thr-pro-leu-arg-ser-lys-lys-thr-met-leu-val-gln-lys-asn-val
27 42↑43 N 52
thr-ser-glu-ser-thr-cys-cys-val-ala-lys-ser-tyr-asn-arg-val-thr-val-met-gly-gly-phe-lys-val-glu-asn-
54 78
his-thr-ala-cys-his-cys-ser-thr-cys-tyr-tyr-his-lys-ser
79 92

β-subunit, molecular weight: 15,532 (peptide) + 8,351 (carbohydrate)

N N
ser-lys-glu-pro-leu-arg-pro-arg-cys-arg-pro-ile-asn-ala-thr-leu-ala-val-glu-lys-glu-gly-cys-pro-val-cys-ile-thr-val-asn-
1↑2 13 30
thr-thr-ile-cys-ala-gly-tyr-cys-pro-thr-met-thr-arg-val-leu-gln-gly-val-leu-pro-ala-leu-pro-gln-val-val-cys-asn-tyr-arg-
31 43↑44↑45 47↑48
asp-val-arg-phe-glu-ser-ile-arg-leu-pro-gly-cys-pro-arg-gly-val-asn-pro-val-val-ser-tyr-ala-val-ala-leu-ser-cys-gln-cys-
61 75↑76
ala-leu-cys-arg-arg-ser-thr-thr-asp-cys-gly-gly-pro-lys-asp-his-pro-leu-thr-cys-asp-asp-pro-arg-phe-gln-asp-ser-ser-ser-
O O O O
ser-lys-ala-pro-pro-pro-ser-leu-pro-ser-pro-ser-arg-leu-pro-gly-pro-ser-asp-thr-pro-ile-leu-pro-gln
121 127 132 138 145

Fig. 1. The primary structure of the α- and β-subunits of hCG with carbohydrate attachment sites *(49)*. Numbers are amino acid sequence order. N indicates asparagine residues with N-linked oligosaccharide, and O indicates serine residues with O-linked glycans. Arrows (↑) denote sites of potential amino-terminal heterogeneity and nicking of internal peptide bonds. Molecular weight for α-subunit calculated based on an intact primary sequence, five disulfide bonds, one sialylated monoantennary and one sialylated biantennary N-linked oligosaccharide. Molecular weight for β-subunit calculated based on an intact primary sequence, six disulfide bonds, one sialylated biantennary and one sialylated, fucosylated biantennary N-linked oligosaccharide, and four sialylated, disaccharide-core O-linked oligosaccharides.

promoting steroidogenesis *(1,2)*. During the early weeks of pregnancy, the trophoblast secretion of hCG stimulates ovarian production of progesterone, both hormones being critical to successful implantation and maintenance of the fetal graft. Additional, less-defined properties of hCG include immuno- and invasion-suppressive activities *(3,4)*.

hCG is composed of two dissimilar subunits, designated α and β. The primary sequence of α-subunit consists of 92 amino acids with 5 disulfide bonds and N-linked carbohydrate attachment sites at asparagine residues α52 and α78. Biological activity is conferred upon noncovalent association with β-subunit *(5)*. The peptide portion of β-subunit consists of 145 amino acids with 6 disulfide bonds and N-linked carbohydrate attachment sites at asparagine residues β13 and β30 *(5,6)*. The most striking difference between the protein sequence of the β-subunit of hCG and those of the other glycoprotein hormones (LH, TSH, FSH) is the inclusion of a 25- to 30-residue carboxy-terminal extension. O-linked carbohydrate attachment sites are located on this serine/proline-rich domain at serine residues β121, β127, β132, and β138 (Fig. 1).

The carbohydrate processing pathway of hCG resembles that of other secretory glycoproteins: in the endoplasmic reticulum, precursor oligosaccharide is transferred to two asparaginyl residues of each nascent α- and β-peptide chain *(7,8)*; as the combined αβ dimer is transported through the Golgi, glycosidase and glycosyltransferase activities complete the processing of N-linked oligosaccharide and the addition of O-linked oligosaccharide to the β carboxy-terminal extension *(9–11)*. The processes that lead to this heterodimer with final glycosylation at eight sites are complex, involving the critical folding of β-subunit both before and after combination with α-subunit *(12)*. The recent determination of the crystal structure of hCG indicates a cystine-knot motif similar to the core regions of platelet-derived and transforming growth factors *(6)*. Since hCG is produced in normal, hyperplastic, and malignant cells, it is a potential marker of cellular change and, as such, is of particular interest as a model for investigating the processes of a normal invasive state (pregnancy) vs those of a malignant condition.

Peptide heterogeneity has been reported at the amino-terminus of α-subunit and, in β-subunit, peptide-bond cleavages ("nicking") have been identified *(13–17)*. In the carbohydrate moiety, numerous permutations have been reported in both the N- and the O-linked glycans of hCG

from normal pregnancy *(18–24)*.* In hCG from choriocarcinoma, unusual N-linked biantennary and triantennary glycans *(25)* with extreme variation in the sialic acid content *(26)* and increased O-linked tetrasaccharide-core structure have been reported *(23,24)*. Progressive changes in the glycosylation content of the hCG produced as pregnancy advances have also been described *(27–29)*. The carbohydrate moiety has been shown to be essential for the biological activity of hCG; complete or partial removal of the N-linked oligosaccharides abolishes steroidogenesis, although the precise nature of the structural involvement remains uncertain *(30)*.

Previous structural studies of hCG that focused on carbohydrate heterogeneity or on peptide integrity have been limited to a few individual samples (purified and analyzed by differing methodologies), to CR standard preparations of hCG, or to subunit preparations purified from proprietary crude extracts of pooled pregnancy urine. The assessment of inherent heterogeneity is difficult when both varied results and differing protocols are reported, while the isolation of hCG from commercial extracts raises concerns regarding the inclusion of urine from abnormal pregnancies, and the preferential selection or deletion of certain forms of heterogeneity in the initial, unknown stages of purification. In addition, any investigation of hCG purified from pooled samples cannot address the issue of heterogeneity, which is attributable to individual variation. The purpose of this study was to describe more thoroughly the combined peptide and carbohydrate heterogeneity of hCG. To this aim, we sought:

1. To analyze an increased number of samples from individuals to assess that level of heterogeneity owing solely to individual variation;
2. To compare directly hCG from normal and aberrant states of pregnancy and from choriocarcinoma, all purified in the same manner;
3. To separate hCG into its respective α- and β-subunits for improved resolution of data;
4. To examine both the peptide-sequence integrity and the accompanying N- and O-linked carbohydrate structures; and
5. To address any concurrent peptide–carbohydrate relationship.

Results

Purification of hCG α- and β-Subunits

hCG was isolated from 14 separate urine collections obtained from individuals with normal pregnancy, diabetic pregnancy,** hydatidiform mole, or choriocarcinoma and then tested for purity as described in Materials and Methods. In addition, two standard preparations (CR127 and CR129 hCG) were investigated. Following the dissociation and resolution of the hCG into its constituent α- and β-subunits, the integrity of the respective subunit pools was assessed for nondissociated hCG and for the alternative subunit using hCG- and subunit-specific immunoassays. The determined mean values were as follows: for the α-pools, 0.4% hCG- and 2.7% β-immunoreactivity, and for the β-pools, 2.2% hCG- and 1.8% α-immunoreactivity. Amino-terminal sequence analysis revealed only α-subunit sequences in the reduced and S-carboxymethylated (RCM) α-preparations and only β-subunit sequences in the RCM β-subunit preparations.

Determination of Amino-Terminal Heterogeneity and Peptide-Bond Nicking

In an earlier study by this laboratory, heterogeneity was detected at the amino-terminus of α-subunit at α3 and α4, but solely in hydatidiform mole and choriocarcinoma hCG *(14)*. Internal peptide-bond nicking was identified at two sites: β44–45 and β47–48. The earlier study was limited by the inherent difficulty in resolving overlying α- and β-subunit sequences in the nondissociated hCG preparations, plus the presence of additional amino-terminal sequences if either or both subunits were internally nicked. In this study, 16 purified hCG samples were separated by dissociation and size exclusion into their respective α- and β-subunits, and then reduced and S-carboxymethylated prior to amino-terminal sequence analysis. This approach allowed greater resolution of peptide heterogeneity specific to the individual subunits and resulted in the detection of additional nicking sites. Sequence analysis revealed that 14 of 15 RCM α-subunits exhibited heterogeneity at the amino-terminus, with 6–18% of the molecules commencing at α3 and/or α4 (Table 1). The extent of amino-terminal heterogeneity for α-subunit was similar in all categories examined: for the four individual and two CR standard preparations from normal pregnancy (mean: 9.4 and 11.1%, respectively), for diabetic pregnancy (sample D1, 6.5%), for the three hydatidiform mole (7.9%), and for the four choriocarcinoma (12.6%) individual samples. For β-subunit, only 1 of 15 samples, choriocarcinoma C7, exhibited any amino-terminal heterogeneity (40.5% commencing at β2).

Internal peptide-bond nicking was detected in 2 of 15 α-subunits (CR129 standard preparation and choriocarcinoma C2). Both were nicked at a previously unreported site, between α42–43 (4 and 19%, respectively) (Table 1). In β-subunit, internal nicking was detected in 12 of 15 subunits tested. As in the earlier study *(14)*, cleavage

*Complex-type asparagine (N)-linked oligosaccharide structure is classified according to the number of antennae or branches attached to the $Man_3GlcNAc_2$ core (e.g., mono-, bi-, tri, tetra-antennary) and is designated herein according to the sugar present at the desialylated nonreducing terminus using the following code: G, Galactose; M, Mannose; A, *N*-acetylglucosamine. The presence of core fucose (attached to the GlcNAc linked to asparagine) is designated by F. Serine (O)-linked oligosaccharides are classified according to the number of neutral sugar residues (e.g., di-, tetra-saccharide).

**Diabetes prior to and during pregnancy.

Table 1
Amino-Terminal Heterogeneity and Internal Peptide-Bond Nicking in Separated RCM α- and β-Subunits

	Amino-terminal sequences detected in α starting at[a]					Amino-terminal sequences detected in β starting at[a]							
Sample code	α1	α3	α4	Total[b] α3, 4	α43	β1	β2	β44	β45	β48	β76	Total β44, 45, 76	Total[c] β44–76
Normal pregnancy													
Standard CR127	1.0	0.02	0.12	0.14	0	1.0	0	0	0.07	0.12	0	0.07	0.19
Standard CR129	1.0	0	0.11	0.11	0.04	1.0	0	0	0.04	0	0	0.04	0.04
Individual P3	1.0	0	0.08	0.08	0	1.0	0	0	0	1.04	0	0	1.04
Individual P7	1.0	0.22	0	0.22	0	nd[d]	nd	nd	nd	nd	nd	nd	nd
Individual P8	1.0	0	0.07	0.07	0	1.0	0	0	0	0	0	0	0
Individual P9	1.0	0	0.06	0.06	0	1.0	0	0	0	0	0	0	0
Diabetic pregnancy													
Individual D1	1.0	0.07	0	0.07	0	1.0	0	0	0	0	0	0	0
Individual D2	1.0	0	0	0	0	1.0	0	0	0	0.08	0	0	0.08
Hydatidiform mole													
Individual M1	1.0	0.06	0	0.06	0	1.0	0	0.09	0	0.09	0.06	0.15	0.24
Individual M2	1.0	0.05	0.07	0.12	0	1.0	0	0.04	0	0.03	0.08	0.12	0.15
Individual M4	1.0	0	0.08	0.08	0	1.0	0	0	0	0.98	0	0	0.98
Choriocarcinoma													
Individual C1	1.0	0.06	0.12	0.18	0	1.0	0	0.12	0.17	0.08	0	0.29	0.37
Individual C2	1.0	0	0.15	0.15	0.19	1.0	0	0	0.27	0.16	0	0.27	0.43
Individual C3	1.0	0.09	0	0.09	0	1.0	0	0.05	0.07	0.13	0	0.12	0.25
Individual C5	1.0	0.03	0.13	0.16	0	1.0	0	0	0	1.06	0	0	1.06
Individual C7	nd	nd	nd	nd	nd	1.0	0.68	0	0.03	0	0	0.03	0.03

[a]Sequences were determined from a minimum of eight cycles of analysis. Finding a sequence required identification in at least four of the first six consecutive residues with comparable levels (within 50%). Finding at least two unique residues (those not in any other sequence) was also a requirement. Concentrations of at least two unique residues were used to estimate amounts of sequences. These were Val 4 and Pro 2 for α1, Val 2 and Gln 3 for α3, Gln 2 and Pro 5 for α4, and Lys 2 and Lys 3 for α43. The unique residues were Pro 4 and Lys 2 for β1, Leu 4 and Arg 5 for β2, Gln 3 and Gly 4 for β44, Gln 2 and Gly 3 for β45, Ala 4 and Gln 6 for β48, and Asn 2 and Val 5 for β76. Molar values were normalized to the concentration of sequence starting at residue 1.

[b]Total amino-terminal heterogeneity = sum of all normalized sequences that do not begin at residue 1 (for α-subunit, α3 and/or α4; for β-subunit, β2). Percent amino-terminal heterogeneity = total amino-terminal heterogeneity divided by total normalized sequences ×100. Example: P7α amino-terminal heterogeneity = 0.22 divided by 1.22 (1.00 plus 0.22) × 100 = 18%.

[c]Total internal peptide-bond nicking = sum of all normalized sequences that begin at residue α43 for α-subunit; sum of all normalized sequences that begin at residues β44, β45, β48, and β76 for β-subunit. Percent peptide bond nicked at a particular site = normalized value for nick site ×100.

[d]nd = not determined.

between residues β47-48 was the site of greatest potential for nicking and was detected in all categories. Nicking at β47-48 varied from 0–1.06, but tended to group at the extremes of the range. Nicking was also identified between residues β44-45, and at two new sites, β43-44 and β75-76. With the exception of 7 and 4% nicking at β44-45 in CR127 and CR129 standard preparations, internal nicking at sites other than β47-48 was confined to hydatidiform mole and choriocarcinoma. In hydatidiform mole, β-subunit was nicked at β47-48, and at two new sites: β43-44 and β75-76. Choriocarcinoma β-subunit was nicked at β47-48 as in pregnancy, at β44-45 as in CR standard preparations, and at β43-44 as in hydatidiform mole.

The finding of β-subunit sequences starting at β44, β45, and β48 shows the presence of extra amino termini, but does not prove that prior residues (-β43, -β44, and -β47) are present. Carboxypeptidase Y carboxyl-terminal sequence analysis was used to address this issue. β-subunit preparations M4 and C5 are near-equal mixtures of peptides starting at β1 and β48 (Table 1). This was interpreted as the occurrence of 100% nicking between β47-48. Carboxypeptidase Y released Gly, Gln, Pro, and Leu in the approximate ratio of 1:2:1:2 from both M4 and C5 β-subunit preparations (not shown). This is consistent with the release of three carboxy-terminal amino acids (Gln 145, Pro 144, and Leu 143) from peptide β48–145 and three carboxy-terminal amino acids (Gly 47, Gln 46, and Leu 45) from peptide β1–47. The collective data from the amino- and carboxy-terminal sequence analyses are consistent with little, if any, loss of amino acids from peptides β1–47 or

Table 2
Asparagine-Linked Oligosaccharides of RCM hCG α-Subunit

Sample code	GM, %	GGF, %	GGM, %	GG, %	GGGF, %	GGG, %	Sialic acid, pmol/pmol oligosaccharide I %[a]	
Normal pregnancy								
Standard CR127	48.0	8.9[b]	0	38.4[b]	0[c]	4.8[c]	1.50	95.6[d]
Standard CR129	49.7	3.1	0	37.8	0	9.4	1.47	91.9
Individual P3	53.8	7.3	0	36.4	2.6	0	1.76	117.9
Individual P7	40.7	7.9	0	37.1	14.3	0	1.70	98.2
Individual P8	41.5	7.3	0	41.1	10.1	0	1.73	102.8
Individual P9	61.9	9.4	0	29.2	0	0	1.44	103.4
Diabetic pregnancy								
Individual D1	12.0	7.0	34.8	24.2	22.0	0	0.71	33.7
Individual D2	28.3	2.8	34.0	17.1	17.7	0	0.93	49.2
Hydatidiform mole								
Individual M1	43.4	16.7	0	32.3	3.6	3.9	1.32	80.3[d]
Individual M2	53.1	4.4	0	36.6	0	5.9	1.38	90.0
Individual M4	35.7	0	nd[e]	54.6	0.5	9.2	1.39	79.9
Choriocarcinoma								
Individual C1	38.5	16.0[b]	3.6	18.9[b]	6.2	16.7	1.70	92.2[d]
Individual C2	56.6	24.2	3.7	5.7	0	9.8	1.36	88.9
Individual C3	71.1	19.1	2.2	4.9	0	2.9	1.06	80.3
Individual C5	74.8	18.2	2.3	3.5	0	1.2	0.92	73.1
Individual C7	56.5	20.3	5.1	6.8	8.0	4.3	0.98	61.9

[a]Percent = pmol sialic acid/(pmol GM) + 2 (pmol GG, GGM, and GGF) + 3 (pmol GGG and GGGF).
[b]Biantennary oligosaccharides contain additional fucose in hCG α-subunit from choriocarcinoma. GGF levels are raised in choriocarcinoma vs normal pregnancy (*t*-test: $P < 0.0001$) and in choriocarcinoma vs hydatidiform mole plus normal pregnancy (*t*-test: $P < 0.0001$). GG levels are lowered in the same comparisons ($P < 0.0001$ and $P < 0.0001$, respectively).
[c]In *t*-tests, no significant difference in proportion of triantennary oligosaccharides (GGGF plus GGG) in hCG α-subunit between normal pregnancy vs choriocarcinoma or in normal pregnancy plus hydatidiform mole vs choriocarcinoma ($P > 0.05$).
[d]In hCG α-subunit, sialic acid content is reduced in choriocarcinoma vs normal pregnancy (*t*-test: $P < 0.01$) and in hydatidiform mole vs normal pregnancy (*t*-test: $P < 0.01$).
[e]nd = not determined.

β48–145 and with the single cleavage of peptide linkage between β47-48. Choriocarcinoma sample C2 has peptides starting at β45 (27%) and β48 (16%), indicating nicks between β44-45 and β47-48 (Table 1). The possibility was considered that the three intervening amino acids (β45, 46, and 47) could be missing in a portion of molecules. If this were true, up to 43% (27 plus 16%) of the molecules could terminate at Val 44 and up to 16% could be missing β45–47. Carboxypeptidase Y released Gly, Gln, Pro, Leu, and Val from RCM β-subunit C2 in the approximate ratio of 0.04:1:1:1:0.4 (not shown). This was consistent with the release of Gln 145, Pro 144, and Leu 143 from the carboxy-terminus of the distal peptide (β48–145), and with the release of Gly 47 at 4% and Val 44 at 40% of the carboxy-terminus of the proximal peptides (β1→|βx). This was consistent with the absence of residues β45, 46, and 47 in 12% (16 minus 4%) of the molecules.

Oligosaccharide Structure in hCG α- and β-Subunits from Normal Pregnancy

α-Subunit from normal pregnant individuals and from standard preparations was characterized by a predominant pair of N-linked oligosaccharides: fucose-free mono-antennary (GM: 49.3 ± 7.9%, mean ± SD) and fucose-free biantennary (GG: 36.7 ± 4.0%) (Table 2). In addition, low but distinct levels of more highly branched structures, fucosylated biantennary (GGF: 7.3 ± 2.2%) and tri-antennary oligosaccharides (GGG plus GGGF: 6.9 ± 5.3%), were also identified. The oligosaccharides of α-subunit from normal pregnancy contained 101 ± 9.1% sialylated antennae.

β-Subunit from normal pregnancy hCG contained a predominant pair of biantennary N-linked oligosaccharides: GGF (50.8 ± 8.0%) and GG (30.9 ± 6.6%) (Table 3). In addition, distinct levels of monoantennary (GM: 4.6 ± 2.7%) and triantennary (GGG plus GGGF: 13.7 ± 5.9%) oligosaccharides were identified. The sialylation of the N-linked oligosaccharides was near complete at 98.2 ± 5.5% sialylated antennae. The O-linked oligosaccharide of β-subunit was predominantly disaccharide-core structure (84.5 ± 2.8%), but a significant level (15.6 ± 2.8%) of more highly branched tetrasaccharide-core structure was also detected (Table 4). The extent of sialylation was not complete in the O-linked glycans, at 62.9 ± 13.7% sialylated antennae.

Table 3
Asparagine-Linked Oligosaccharides of RCM hCG β-Subunit

Sample code	GM, %	GGF, %	GGM, %	GG, %	GGGF, %	GGG, %	Sialic acid, pmol/pmol oligosaccharide	%
Normal pregnancy								
Standard CR127	3.6[b]	56.3[b]	0	34.7[b]	5.4[b]	0[b]	1.91	94.5[c]
Standard CR129	2.2	59.3	0	27.7	10.8	0	2.01	96.3
Individual P3	6.5	44.3	0	38.9	8.3	2.1	2.00	97.8
Individual P7	4.4	54.9	0	23.0	13.2	4.5	2.32	108.8
Individual P8	1.9	51.9	0	24.6	17.4	4.2	2.06	93.8
Individual P9	8.8	38.2	0	36.4	12.1	4.4	2.03	97.9
Diabetic pregnancy								
Individual D1	3.8	11.7	43.9	20.7	17.5	2.4	1.04	47.9
Individual D2	6.5	44.3	25.9	13.0	8.3	2.1	2.00	97.8
Hydatidiform mole								
Individual M1	5.5[b]	57.2[b]	nd[d]	19.1[b]	16.5[b]	1.7[b]	2.10	98.5
Individual M2	6.9	38.4	0	22.6	20.9	11.1	2.07	92.0
Individual M4	8.1	22.8	0	39.0	18.5	11.5	2.66	119.8
Choriocarcinoma								
Individual C1	6.8[b]	14.8[b]	0	14.8[b]	52.2[b]	11.4[b]	2.37	92.2[c]
Individual C2	5.9	23.4	0	22.6	38.0	10.1	1.82	75.2
Individual C3	16.4	23.8	0	11.7	33.6	14.5	2.35	101.3
Individual C5	15.9	31.9	0	4.4	42.7	5.1	2.19	94.6
Individual C7	10.9	24.4	9.1	7.5	35.2	12.9	1.60	67.5

[a]Percent = pmol sialic acid/(pmol GM) + 2 (pmol GG, GGM, and GGF) + 3 (pmol GGG and GGGF).

[b]A shift occurs from biantennary to mono- and triantennary oligosaccharides in hCG β-subunit from choriocarcinoma. GGF and GG proportions are lowered in choriocarcinoma vs normal pregnancy (*t*-tests: $P < 0.0001$ and $P < 0.001$) and choriocarcinoma vs hydatidiform mole plus normal pregnancy (*t*-tests: $P < 0.001$ and $P < 0.001$); GM, GGG, and GGGF proportions are raised in choriocarcinoma vs normal pregnancy (*t*-tests: $P < 0.01$, $P < 0.001$, $P < 0.0001$) and choriocarcinoma vs hydatidiform mole plus normal pregnancy (*t*-tests: $P < 0.01$, $P < 0.01$, $P < 0.0001$). A trend is present: GGF and GG proportions decrease in hydatidiform mole and decrease further in choriocarcinoma (Bartholomew's test of increasing means, $P = 0.001$ and $P = 0.002$), and proportions of GM ($P = 0.017$) and triantennary oligosaccharides (GGG and GGGF) are increasingly raised in these conditions ($P < 0.001$).

[c]In *t*-test, sialic acid content in hCG β-subunit for normal pregnancy vs choriocarcinoma, $P = 0.043$.

[d]nd = not determined.

Evaluating the N-linked oligosaccharides in hCG from normal pregnancy, 14.2% of α-subunit and 13.7% of β-subunit glycans were hyperglycosylated (fucosylated and/or triantennary), compared to their predominant subunit-specific carbohydrate structures. Additionally, in the O-linked glycans of β-subunit 15.6% of glycans were hyperglycosylated (tetrasaccharide-core structure).

Oligosaccharide Structure in hCG α- and β-Subunits from Hydatidiform Mole and Choriocarcinoma

Hydatidiform mole α-subunit contained the fucose-free, monoantennary and biantennary structures (GM: 44.1 ± 8.7% and GG: 41.2 ± 11.8%) at similar levels to those of normal pregnancy (Table 2). Fucosylated biantennary (GGF: 7.0 ± 8.7%) and triantennary (GGG plus GGGF: 7.7 ± 1.9%) oligosaccharides were also detected. In choriocarcinoma α-subunit, a significant decrease in fucose-free biantennary GG (to 8.0% ± 6.2%), a major component of normal pregnancy and hydatidiform mole, was accompanied by a significant increase in fucosylated biantennary GGF (to 19.6 ± 3.0%). In all *t*-tests comparing the relative proportions of GG and GGF in normal pregnancy vs choriocarcinoma or normal pregnancy plus hydatidiform mole vs choriocarcinoma, $P < 0.0001$. For samples from individuals, the total triantennary content in α-subunit from choriocarcinoma matched that of normal pregnancy and hydatidiform mole, while fucose-free triantennary GGG was found only in hydatidiform mole or choriocarcinoma. The sialic acid content of oligosaccharide in α-subunit was reduced for hydatidiform mole and choriocarcinoma, with 83.4 ± 5.7 and 79.3 ± 12.3% sialylated antennae (*t*-tests: normal pregnancy vs hydatidiform mole or normal pregnancy vs choriocarcinoma, $P < 0.01$).

For β-subunit N-linked oligosaccharides, a different pattern is apparent. While biantennary GGF and GG were the predominant glycans in normal pregnancy accompanied by distinct levels of mono- and triantennary components, the proportions of the mono- and triantennary oligosaccharides (GM, GGG plus GGGF) increased stepwise from normal pregnancy to hydatidiform mole to choriocarcinoma. Both major glycoforms of normal pregnancy (GGF and GG) were reduced in this trend. The increases

Table 4
Serine-Linked Oligosaccharides on RCM hCG β-Subunit

Sample code	GalNAc	GlcNAc, pmol/pmol[a]	Gal, pmol/pmol[a]	Disaccharide core, %[b]	Tetrasaccharide core, %[b]	Sialic acid, pmol/pmol GalNAc[c]	Sialic acid, %[c]
Normal pregnancy							
Standard CR127	1.0	0.185	1.160	81.5[d]	18.5[d]	1.32	66.0[e]
Standard CR129	1.0	0.156	1.115	84.4	15.6	1.25	62.5
Individual P3	1.0	0.123	1.123	87.7	12.3	1.62	81.0
Individual P7	1.0	0.190	1.180	81.0	19.0	1.02	51.0
Individual P8	1.0	0.125	1.146	87.5	12.5	1.46	73.0
Individual P9	1.0	0.154	1.136	84.6	15.4	0.88	44.0
Diabetic pregnancy							
Individual D1	1.0	0.180	1.144	82.0	18.0	0.69	34.5
Individual D2	1.0	0.186	1.191	81.4	18.6	0.62	31.0
Hydatidiform mole							
Individual M1	1.0	0.111	1.128	88.9[d]	11.1[d]	0.45	22.5[e]
Individual M2	1.0	0.381	1.399	61.9	38.1	0.80	40.0
Individual M4	1.0	0.197	1.157	80.3	19.7	0.98	49.0
Choriocarcinoma							
Individual C1	1.0	0.666	1.679	33.4[d]	66.6[d]	0.52	26.0[e]
Individual C2	1.0	0.479	1.502	52.1	47.9	1.14	57.0
Individual C3	1.0	0.882	1.881	11.8	88.2	0.97	48.5
Individual C5	1.0	1.034	2.064	0	103	1.15	57.5
Individual C7	1.0	0.681	1.678	31.9	68.1	1.05	52.5

[a]Data normalized to 1.0 GalNAc. Values are pmol GlcNAc (determined as glucosamine) per pmol GalNAc (determined as galactosamine), and pmol Gal per pmol GalNAc.

[b]Previously, two O-linked core structures have been identified as attached to β-subunit of hCG: Galβ1,3GalNAc-O~ (disaccharide core) and Galβ1,3(Galβ1,4GlcNAcβ1,6)GalNAc-O~ (tetrasaccharide core) *(23,24)*. The total concentration of both structures was determined by the amount of GalNAc ($n = 1$). The proportion of tetrasaccharide core was determined by the concentration of GlcNAc ($n = 1$) and confirmed by the concentration of Gal ($n = 2$).

sample P7:	GalNAc	GlcNAc	Gal
	1.000 ($n = 1$)	0.190 ($n = 1$)	1.180
	−0.190		−0.380
	0.810 ← (×100 = % disaccharide) → 0.800		

[c]Data are pmol sialic acid per pmol GalNAc. Both the di- and tetrasaccharide core structures can have two sialic acid residues. Percent sialic acid = pmol/pmol divided by 2 × 100.

[d]Proportions of disaccharide core decrease and tetrasaccharide core increase in choriocarcinoma vs normal pregnancy (*t*-tests: $P < 0.0001$ and $P < 0.0001$). A trend is present: proportions of tetrasaccharide core increase in hydatidiform mole and increase further in choriocarcinoma (Bartholomew's test of increasing means, $P < 0.001$), and proportions of disaccharide core are increasingly lowered in these conditions ($P < 0.001$).

[e]Sialic acid content of O-linked glycans in β-subunit from choriocarcinoma vs normal pregnancy (*t*-test: $P = 0.052$) and hydatidiform mole vs normal pregnancy (*t*-test: $P = 0.016$).

were: for monoantennary oligosaccharide, from 4.6 ± 2.6 to 6.8 ± 1.3 to 11.2 ± 4.9% and, for triantennary, from 13.7 ± 5.9 to 26.7 ± 7.5 to 51.5 ± 6.8%.

A trend was also identified in the O-linked oligosaccharide of β-subunit: tetrasaccharide-core structure increased from 15.6 ± 2.8% in normal pregnancy to 23.0 ± 13.8% in hydatidiform mole, to the predominant level of 74.8 ± 21.3% in choriocarcinoma. An increasing trend is shown for the mono- and triantennary N-linked oligosaccharides, and for the tetrasaccharide-core *O*-glycans (Bartholomew's tests of increasing means, $P = 0.017$, $P < 0.001$, and $P < 0.001$, respectively). There was no accompanying stepwise trend (normal pregnancy to hydatidiform mole to choriocarcinoma) in the total fucose content of β-subunit (62.0 ± 8.7, 58.1 ± 16.2, 64.0 ± 6.9%), in the sialic acid content of the N-linked oligosaccharides (98.2 ± 5.5, 103 ± 14.5, and 86.2 ± 14.2% sialylated antennae), or in the sialic acid content of the O-linked glycans (62.9 ± 13.7, 37.2 ± 13.5, and 48.3 ± 13.0% sialylated antennae).

Evaluating the N-linked oligosaccharides in hCG from hydatidiform mole and choriocarcinoma, 14.7 and 29.4% of α-subunit and 26.7 and 51.5% of β-subunit glycans were hyperglycosylated (triantennary) compared to the subunit-specific carbohydrate structures of normal pregnancy. Additionally, in O-linked β-subunit, 23.0 and 74.8% of glycans were tetrasaccharide-core structure.

Determination of Oligosaccharide Structure in hCG α- and β-Subunits from Diabetic Pregnancy

For the two α-subunits purified from diabetic pregnancy hCG, an unusual biantennary structure, GGM, was the major N-linked oligosaccharide (34.4%, mean) (Table 2). The predominant components of α-subunit from normal pregnancy decreased in diabetic pregnancy (to 20.2% for GM and 20.7% for GG). Fucose-containing biantennary (GGF: 4.9%) and triantennary (GGGF: 19.9%) oligosaccharides were also identified, with GGGF being elevated compared to normal pregnancy. In β-subunit, GGM (34.9%) was a major component (as it was in α-subunit) and, for O-linked glycans, a significant level of tetrasaccharide-core structure (18.3%), similar to that of normal pregnancy, was found (Table 4). The sialic acid content of N-linked glycans was notably reduced in diabetic pregnancy hCG. In α-subunit, both samples were <50% sialylated (33.7 and 49.2%), whereas in β-subunit, D1 (Type 1) contained 47.9% and D2 (Type 2), 97.8% sialylated antennae. Similarly, the sialic acid content of the O-linked glycans was notably lower than that found in normal pregnancy (32.8% vs 62.9 ± 13.7% sialylated antennae, respectively).

The following points stand out regarding the oligosaccharide structures of the individual subunits of hCG: (1) normal individual pregnancy samples were found to have significant levels of hyperbranched (i.e., hyperglycosylated) oligosaccharides in addition to their major glycoforms. Specifically, GGF and GGGF were found in α-subunit, whereas GGG, GGGF, and tetrasaccharide-core structure were found in β-subunit. (2) In individuals with choriocarcinoma, the most striking results were all associated with increases in the hyperglycosylated species: for α-subunit, GGF increased over 2.5-fold as one major glycoform decreased; for β-subunit, N-linked GGGF increased over 3.5-fold as both major glycoforms decreased and, for O-linked β-subunit, tetrasaccharide-core structure increased over 4.5-fold as disaccharide-core structure decreased.

Discussion

This study covers the structural heterogeneity of hCG, resolved into its constituent α- and β-subunits, from individuals with normal pregnancy, diabetic pregnancy, hydatidiform mole, or choriocarcinoma. While the results show that the predominance of hCG molecules from normal pregnancy have an intact primary sequence accompanied by subunit-specific oligosaccharide structures, this study also shows that distinct levels of both protein and carbohydrate heterogeneity exist even in *normal* pregnancy hCG, measured here by amino-terminal heterogeneity, internally nicked peptide bonds, and hyperglycosylated oligosaccharide structures. Furthermore, the levels of specific forms of heterogeneity detected in normal pregnancy hCG are shown to increase with the occurrence of abnormal pregnancy or malignant disease.

Hyperglycosylation in hCG α-Subunit (Table 2)

α-Subunit from normal pregnancy hCG had been reported to be specific for fucose-free monoantennary and/or biantennary oligosaccharide (GM, GG). Subsequently, with the use of pulsed-amperometric detection (PAD), 10% of the carbohydrate in α-subunit from second- and third-trimester individual pregnancy hCG and 5%, in CR125 standard preparation were found (by hydrolysis) to be fucosylated *(31)*. In this study, also using PAD and now with the isolation of intact oligosaccharides, we report that fucose is present in α-subunit from standard preparations CR127 and CR129 and, is specifically attributable to biantennary GGF (6.0%, mean). For the normal pregnancy samples, we find that the major glycoforms are fucose-free GM and GG; however, we also observe that 14.2% of the oligosaccharides fall into the hyperglycosylation class for this subunit (total fucosylation, 11.8% and total triantennary, 6.9%). In choriocarcinoma, the α-subunit exhibited increased total hyperglycosylation to 29.4% (total fucosylation, 22.4% and total triantennary, 9.8%) and the most significant change from normal pregnancy to choriocarcinoma was the concordant increase in GGF and decrease in GG ($P < 0.0001$).

Hyperglycosylation in hCG β-Subunit (Tables 3 and 4)

Carbohydrate studies on dissociated β-subunit from normal pregnancy hCG have indicated its specificity for biantennary structures (GG and GGF). An indication of triantennary structure was noted with the detection of ~4% trisialylated structure *(21)*. In the present study, a definitive level of triantennary structure was detected in the normal pregnancy samples (total triantennary, 13.7%). Total triantennary content increased thusly: normal pregnancy = diabetic pregnancy < hydatidiform mole < choriocarcinoma (13.7, 15.2, 26.7, and 51.1%) with the fucose-containing form (GGGF) being relatively higher in each category. Thus, in the comparison of β-subunit from normal pregnancy to choriocarcinoma, triantennary structure becomes the major glycoform and is offset by a parallel decrease in biantennary structure ($P < 0.0001$). Although total fucosylation content did not change significantly in choriocarcinoma vs normal pregnancy in β-subunit, there was a significant shift away from fucosylated biantennary (GGF), the major N-linked oligosaccharide seen in normal pregnancy, to fucosylated triantennary structure (GGGF) in choriocarcinoma ($P < 0.0001$).

Neoplastic transformation, tumor cell invasiveness, and metastatic potential are associated with the presence of hyperbranched, N-linked oligosaccharide. The hyperglycosylation of O-linked glycans involves the "branching enzyme," β1,6GlcNAc transferase, and with the subsequent addition of Gal, results in tetrasaccharide-core structure *(32)*. Hyperglycosylated O-linked structure was identified at significant levels in β-subunit from normal and diabetic pregnancy hCG (15.6 and 18.3%). This extended to upper

limit of the range of tetrasaccharide-core structure detected in normal individual pregnancy hCG *(23,24)* and extended the category of conditions to include that of diabetic pregnancy. Further, we also found a strong correlation for the increase in the tetrasaccharide-core structure in comparing normal pregnancy to choriocarcinoma ($P < 0.0001$). Tetrasaccharide-core structure was the major O-linked oligosaccharide in four of the five choriocarcinoma samples (range: 47.9–103%; mean: 74.8%). These results expand the upper limit of the range for tetrasaccharide-core content detected in β-subunit from choriocarcinoma *(23,24)*.

Sialylation of hCG α- and β-Subunits

The sialic acid content of N-linked oligosaccharide has been reported to range from 90–100% in nondissociated hCG from pooled normal pregnancy samples and CR standard preparations *(26,33)* to <3–100% in choriocarcinoma hCG from individuals *(26)*. The results of the present study confirm near-complete sialylation of the N-linked oligosaccharide from dissociated α- and β-subunits isolated from normal individual pregnancy hCG and the CR standard preparations. In the present study, five samples of choriocarcinoma hCG were examined, and the α-subunit was found to range from 61.9–92.2% sialylation in the N-linked oligosaccharide, statistically reduced vs that of normal pregnancy ($P < 0.01$). The sialic acid content in the N-linked carbohydrate of β-subunit from choriocarcinoma ranged from 67.5–101%. However, the two choriocarcinoma samples that were complicated by hyperthyroidism, C2 and C7, accounted for the decreased sialic acid content in this category; thus, the remaining choriocarcinoma samples contained nearly complete sialylation on their N-linked antennae.

With the investigation of the oligosaccharide structure of the first two samples of hCG from diabetic pregnancy, it is still early in the structural study of this potential accompanying condition to pregnancy and its effect on the heterogeneity of hCG. The samples examined in this study represent different types of diabetes: Type 1, characterized by insulin dependence with the potential for high blood glucose levels during pregnancy, and Type 2, a less severe condition with increased insulin secretion or insulin resistance in target tissues. The antennae of the N-linked oligosaccharides in two α- and one β-subunit were <50% sialylated, while the O-linked sialic content in both β-subunits was in the lower range compared to all other samples. Initial carbohydrate results include a structure (GGM) consistent by composition and mass spectrometry with a glycoform reported previously only in choriocarcinoma hCG and γ-glutamyltranspeptidase produced in hepatocellular carcinoma *(26,34)*. This structure is the predominant N-linked glycoform (34.4 and 34.9%, means) in both the α- and β-subunits of the 2 hCG samples from diabetic pregnancy and was otherwise only found here in the choriocarcinoma samples.

This examination of peptide and carbohydrate heterogeneity has been greatly aided by the use of dissociated hCG and recent technology with increased sensitivity to improve detection of low levels of additional carbohydrate heterogeneity. Further, by using a larger number of samples, which were purified using the same methodology, we can begin to establish the ranges of heterogeneity attributable to individual variation. This becomes very important in trying to define both what indicates and what produces a disease state. In the protein moiety, α-subunit amino-terminal heterogeneity has been extended to include the category of first-trimester normal pregnancy. In addition to the known β-subunit nick sites at β44-45 and β47-48 *(14)*, additional nicked linkages have been found at β43-44 in hydatidiform mole and choriocarcinoma, at β75-76 in hydatidiform mole, and at α42-43 in α-subunit. In the carbohydrate moiety, the use of individual subunits made it possible to assign the lower levels of glycoforms to specific subunits and to observe changes in the various categories, many of which would not be found with nondissociated hCG analyses. A most significant example is the comparison of GGF from normal pregnancy vs choriocarcinoma. If the results found here were recalculated assuming nondissociated hCG, the change for GGF would only be from 29.1 to 21.6%. By looking at individual subunits, it could be seen that GGF actually increased significantly in α-subunit, from 7.3 to 19.6% (2.7-fold increase), while decreasing in β-subunit from 50.8 to 23.7% (53% decrease).

In summary, this study shows that compared to normal pregnancy, the hCG produced by choriocarcinoma has increased levels of N-linked fucosylated (vs fucose-free) biantennary oligosaccharide in α-subunit, fucosylated triantennary (vs biantennary) structure in β-subunit, and tetrasaccharide-core structure at its O-linked carbohydrate sites. All of these suggest either increased access by or increased concentrations of "branching" enzymes (α1,6fucosyltransferase, GlcNAc transferase IV, and β1,6GlcNAc transferase) in malignant disease. Hyperglycosylation is significantly elevated in and potentially indicative of choriocarcinoma, but as seen in the distinct levels of hyperglycosylation in normal pregnancy, this modification is not unique, but rather an amplification in malignant disease.

Carbohydrate–Protein Interactions

Carbohydrate and protein heterogeneity of hCG has been shown to occur in normal pregnancy and to be amplified in choriocarcinoma. In an attempt to analyze these changes, we have examined our results relative to the studies of the hCG folding pathway *(12)* and the recently determined crystal structure *(6)*. Based on the comparisons found here of the glycan changes between the α- and β-subunits from choriocarcinoma vs those of normal pregnancy and on the studies showing the hyperglycosylation of α to largely triantennary structure when it remains uncombined *(31,35)*, we

believe the changes in *N*-glycosylation more likely result from steric considerations rather than from changes in enzyme levels. For example, in choriocarcinoma, GGGF is significantly increased to 40.3% in β-subunit, implying at least moderate levels of α1,6fucosyltransferase, GlcNAc transferase II, and GlcNAc transferase IV. At the same time, in the presence of the same enzyme concentrations, GGGF in α-subunit is at low levels (2.8%). In direct opposition, GM in α-subunit remains very high in choriocarcinoma, actually increasing compared to normal pregnancy from 49.3 to 59.5%, the GM structure being associated with the reduction or lack of the three enzymes just mentioned. A host of such comparisons is easily seen in the data and leads us, therefore, to consider steric effects of at least equal importance, in N-linked glycosylation, to the concept of a change in enzyme levels as the sole source of altered carbohydrate patterns.

With regard to the folding pathway of hCG, the focus is on a dynamic system in which it is likely that folding influences glycosylation, which, in turn, influences new folding, and so on, the process working its way stepwise to a heterogeneous population even in the "normal" situation of "normal" pregnancy. In the synthesis and processing of hCG, α-subunit is synthesized, receiving *en bloc* $Glc_3Man_9GlcNAc_2$ oligosaccharide at αAsn52 and αAsn78, and folds readily into an assembly-competent core, completing all five of its disulfide bonds prior to combination. β-Subunit receives precursor oligosaccharide at βAsn13 and βAsn30, and arrives at its assembly-competent stage more slowly by completion of a complex series of folding intermediates involving its first 3–4 core disulfide bonds *(12)*. The studies have suggested that β-subunit's last two disulfide bonds, 5 and 6, are initially formed, but then reduced to allow for αβ combination, and ultimately reformed as part of the final folding processes. Two additional points emphasize the complexity of the ongoing process: (1) The folding and assembly pathway of hCG shows that the initial αβ-combined stage contains partially unfolded β-subunit with its three latest-forming disulfide bonds (β23-72, β93-100, and β26-110) in various stages of completion *(12)* (Fig. 2A–C); (2) a rearrangement of two of β-subunit's core disulfide bonds may also occur, when comparing immature, initially combined hCG to mature secreted hCG *(6,12)*. All of this suggests a structure that moves through many conformations to attain its final folded and glycosylated state. At a minimum, with a population of αβ-combined subunits entering the Golgi with a distribution of uncompleted or transient disulfide bonds in the β-subunit, a more variable and open conformation provides an environment for heterogeneous glycosylation processing of carbohydrate sites in both α- and β-subunits.

αAsn52 Site

The crystal structure of mature hCG shows significant features for αAsn52 (Fig. 2). First, hydrogen bonding between β99–101 and α53–57 secures its interchain position and, additionally, disulfide bonds β93-100 and β26-110 lock residues β100 to 110 essentially in an arm across the region of αAsn52. Since both hydrogen- and disulfide-bonding features are fundamental to the conformation and accessibility to the αAsn52 site, any events that can alter the complex folding patterns of hCG have the potential to alter its glycosylation. Studies using glycopeptides as antagonists to adenylate cyclase stimulation by the native hormone and those using site-directed mutagenesis have determined a major role for the carbohydrate of α-subunit, specifically at αAsn52, in successful cAMP and steroid production *(36,37)*. Additionally, the absence of disulfide bond β93-100 by in vitro reduction or the site-mutated substitution of Ala for Cys at residues β93 and β100 results in the complete loss of receptor binding *(38,39)*. Additional complexity is added to this region when the putative site of phosphorylation by cAMP-dependent protein kinase is βThr97 *(40)*. Therefore, hyperglycosylation at the αAsn52 site could have effects on both receptor binding and steroidogenesis through impeding proper formation/reformation of disulfide bonds β93-100 and β26-110 or by preventing hydrogen bond formation between β99–101 and α53–57, thus, altering the normal tertiary relationship for signal transduction between the local protein structure, the carbohydrate positioned at αAsn52, and the receptor complex.

αAsn78 Site

Sequence β38–57 is an amphipathic, antiparallel loop implicated in hCG receptor reactions *(39)* (Fig. 2). Residues β34–46 interact with α-subunit through interchain hydrogen bonding, with β44–46 specifically binding to α77–75, immediately adjacent to N-linked oligosaccharide site, αAsn78 (Fig. 2A–C). If hyperglycosylation occurs at αAsn78 and results in the failure to maintain these hydrogen bonds, β38–57 becomes significantly less shielded, and in particular, the apex of this extended receptor loop, β43–48, becomes totally exposed. This is consistent with the findings here of increased internal nicking in this region in hydatidiform mole and choriocarcinoma at multiple sites between β43 and β48, directly concordant with the described hydrogen bonding between β44–46 and α77–75. The presence of hyperglycosylated GGF at αAsn78 may affect hydrogen bonding at β44–46, making this site potentially available to proteases. Functionally, nicking at this apex has been shown to decrease dramatically hCG biological activity, reducing it to 1 or 20% that of intact hCG *(41,42)*.

βAsn13 and βAsn30 Sites

N-linked glycosylation sites, βAsn13 and βAsn30, are positioned in hydrophobic regions of the peptide chain near the amino terminus of β-subunit, interspaced in a cluster of cysteine residues at β9, 23, 26, 34, and 38. In the crystal structure of mature hCG, βAsn13 and βAsn30 colocalize

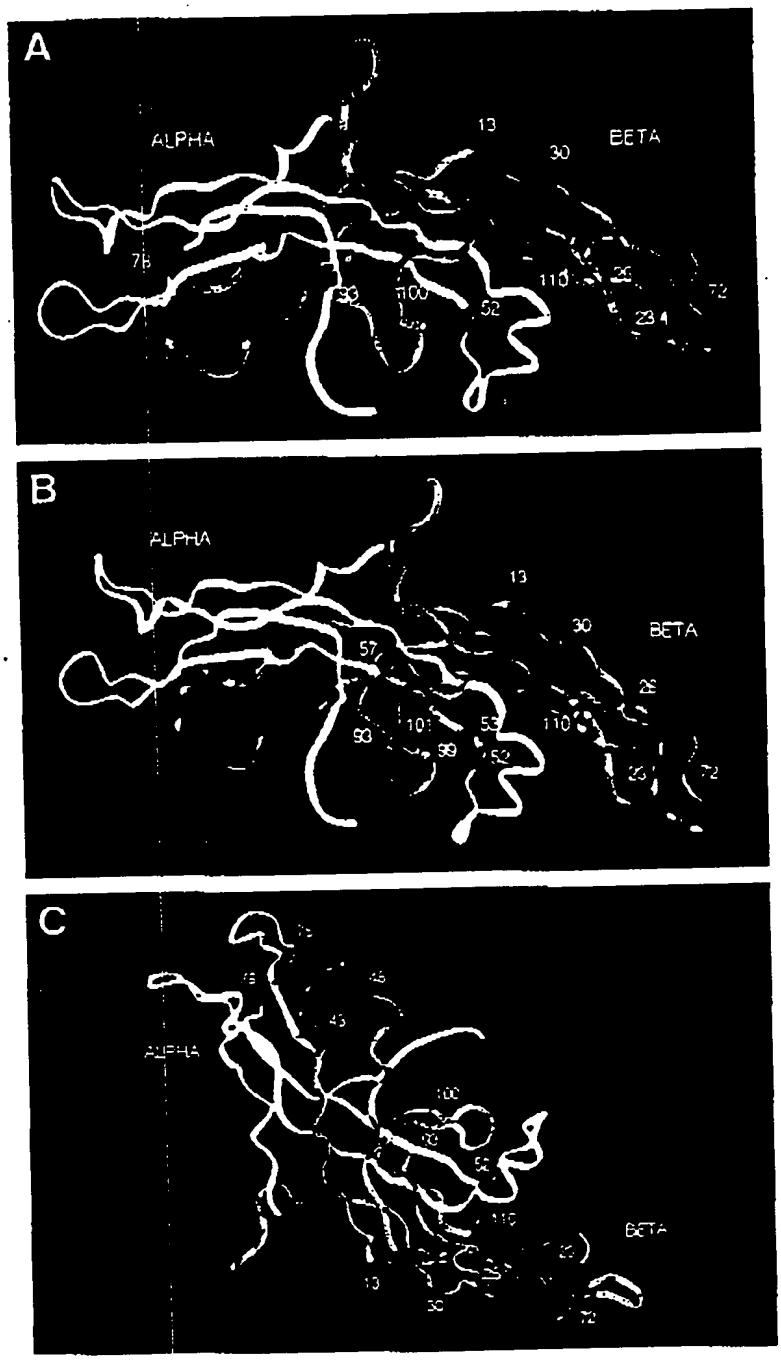

Fig. 2. (A) Ribbon diagram of hCG determined using multiwavelength anomalous diffraction analysis of synchrotron data at 2.6 Å resolution. α-Subunit (residues α5–89) is shown in gold, and β-subunit (residues β2–111), in blue. Three of the 11 intrasubunit disulfide bonds of hCG (latest-forming β23–72, β93–100, β26–110) are shown in purple. N-linked carbohydrate attachment sites (shown in red) are located at αAsn52 and αAsn78 in α-subunit and at βAsn13 and βAsn30 in β-subunit. (B) View of the alignment of interchain hydrogen bonding between sequence α53–57 and sequence β99–101 (both shown in green) with disulfide bond β93–100 (purple) and immediately adjacent, N-linked glycosylation site αAsn52 in α-subunit (red). (C) View of the alignment of interchain hydrogen bonding between sequence α77–75 and sequence β44–46 (both shown in green) with immediately adjacent, N-linked glycosylation site, αAsn78 in α-subunit (red). β-subunit's contribution to this described interchain hydrogen bonding (β44–46) is coincident with the nicking region of β-subunit (β43–48) shown bordered by residues β43 and β48 (in dark blue).

(~7 Å apart), and antiparallel interchain hydrogen bonding occurs between residues β6–8 and α7–5, stabilizing the two amino termini of the combined subunits (Fig. 2). This close spatial relationship would be expected to limit the carbohydrate processing sterically under "normal" conditions, and biantennary structures do predominate. The high level of triantennary hyperglycosylation detected in β-subunit from choriocarcinoma strongly suggests that these events occur when the maturing combined subunits are in a less folded, i.e., "more open" conformation. Regarding biological activity, the level of signal transduction may be affected by the carbohydrate of the β-subunit of hCG. With the site-mutated removal of glycosylation at αAsn52, and with the presence of carbohydrate at βAsn13 or, alternatively, at βAsn30, ~50 or 25% activity is still retained *(37)*. Therefore, the substitution of a mono- or triantennary glycoform for a biantennary structure attached to βAsn13 and/or Asn30 may, in itself, prove to have an effect on steroidogenesis.

βSer121–126, 132, and 138 Sites

Less is known about the steric relationship between the combined αβ intercystine-knot domain and β's carboxy-terminal extension. Multiwavelength anomalous diffraction (MAD) analysis shows residues β112–145 extend off into solution and to be disordered in the crystal *(6)*. Site-mutation studies indicate that the *O*-glycosylation does not influence the efficiency of αβ combination, the extent of heterodimer secretion, or in vitro hCG activity *(43,44)*. Although the carboxy-terminal protein domain is unique to hCG in the glycoprotein hormone family, the mutational removal of residues β111–145 does not significantly affect αβ combination or hCG activity *(45)*. It has been suggested that the carboxy-terminal domain with its O-linked glycosylation confers additional solubility and in vivo circulatory life-time *(44)*. In that the β-subunits of normal pregnancy and choriocarcinoma hCG acquire hyperglycosylated O-linked glycans (tetrasaccharide-core structure: 15.6 and 74.8%), the ratio of tetra- to disaccharide glycosylation may prove to be controlled by the ratio of β1,6GlcNAc transferase to α2,6sialyltransferase, which compete for the same substrate, i.e., disaccharide-core structure *(32)*. The potential contribution of steric effects, if any, to increased tetrasaccharide-core structure is limited by the unavailable three-dimensional data for this region. The large increase in tetrasaccharide-core content seen in choriocarcinoma makes it, at this time, most interesting as a marker for certain precancerous and malignant conditions.

hCG is largely combined upon entering the Golgi, and both subunits are, therefore, exposed to the same glycosylation enzyme concentrations. Since the patterns of glycosylation are so dissimilar when comparing α- to β-subunit, it seems clear that the three-dimensional protein–carbohydrate structure (i.e., one of the substrates) will strongly affect where, and to what extent, a given glycosylation reaction will proceed. We believe that the variations in *N*-glycosylation found here are more consistent with steric limitations ("conformation" of a substrate) than enzyme limitations. Thus, while enzyme levels may be increased in choriocarcinoma, an event, such as the rapid processing of hCG, which is characteristic of this malignant state, can also be envisioned to affect its complex folding patterns and concurrent glycosylation. With the determination of the distribution of glycan structures at the subunit level, a more refined picture of hCG's glycosylation in normal pregnancy and choriocarcinoma has evolved. However, the next refinement will require the specific site location of these glycosylation changes and their individual effects on the biological activities of hCG.

Materials and Methods

Sample Purification

Forty-eight–72 h collections of urine were obtained from 13 individuals: 4 with normal pregnancy, 2 with diabetic pregnancy, 3 with hydatidiform mole, and 4 with choriocarcinoma (Table 5). hCG was purified from these urines using the extraction procedures and chromatography methods described previously *(14)*. During chromatography procedures, attention was given to recovering all hCG with peaks collected to >99% hCG activity (assay sensitivity: ~0.3 ng/mL). The purity of the hCG samples was demonstrated by SDS-PAGE, amino acid analysis, and amino-terminal sequence analysis *(14)*. Sample C7 hCG was purified by John C. Morris of the Mayo Clinic from the urine of a patient with choriocarcinoma (Table 5). Standard reference preparations CR127 hCG and separated CR129 α- and β-subunits were purified by Steven Birken of Columbia University from crude extracts of pooled pregnancy urine (Organon, West Orange, NJ) (Table 5).

To dissociate hCG, preparations CR127 and C7, and the 13 samples purified in this laboratory were reconstituted in 6 *M* guanidine HCl in 0.15 *M* sodium citrate, pH 3.8, and incubated for 3 h at 45°C. Dissociated samples were applied to two tandem columns, 1.6 × 90 cm each, of Sephacryl S-100 HR. To prevent the immediate recombination of α and β, 4 mL of 3 *M* ammonium thiocyanate were applied to the column immediately preceding the dissociated sample, and the subunits were eluted, at 4°C, with 0.1 *M* NH_4HCO_3, pH 7.8. Column fractions were assayed for hCG and for α- and β-subunit activities using EIA assays with antibodies specific for total hCG (2119-12) and total β-subunit (FBT11), and an RIA specific for α-subunit (H7), described previously *(46,14,47*, respectively*)*. Fractions containing any detectable α- or β-subunit immunoreactivity (assay sensitivities: ~0.3 ng subunit/mL) were combined into their respective pools and assessed for purity using hCG- and subunit-specific immunoassays, by reducing SDS-PAGE procedures *(14)*, and by amino-terminal sequence analysis.

Table 5
History of hCG Samples for Subunit Purification and Structural Analysis

Sample code	Diagnosis	Description	Metastases	Sample/standard distributor
CR-series urinary hCG standards				
CR127	IRP Standard[a]	1st–3rd trimester pool		S. Birken, USA
CR129	IRP Standard	1st–3rd trimester pool		S. Birken, USA
From normal pregnancy patient urine				
P3	Singleton	1st trimester (9–9.5 wk)		L. A. Cole, USA
P7	Singleton	1st trimester (8–10 wk)		L. A. Cole, USA
P8	Singleton	1st trimester (8–10 wk)		L. A. Cole, USA
P9	Singleton	1st trimester (8 wk)		S. Rotmensch, USA
From diabetic pregnancy[b] patient urine				
D1	Singleton, type 1	1st trimester (10 wk)		E. Shapiro, USA
D2	Singleton, type 2	1st trimester (8 wk)		E. Shapiro, USA
From spontaneously regressing hydatidiform mole patient urine				
M1	Complete mole	0, 1-d postevacuation		E. Kohorn, USA
M2	Complete mole	Preevacuation		J. Belinson, USA
M4	Complete mole	Preevacuation		E. Kohorn, USA
From choriocarcinoma patient urine				
C1		Pretherapy	Lung, brain	M. Ozturk, USA
C2	With hyperthyroidism	During resistance to therapy	Lung, brain	K. Bagshawe, UK
C3		During resistance to therapy	Lung	K. Yazaki, Japan
C5		Pretherapy	Lung	W. Yixun, China
C7	With hyperthyroidism		Lung	J. C. Morris, USA

[a]International Reference Preparation.
[b]Diabetes prior to and during pregnancy.

Reduction and S-Carboxymethylation

Aliquots of 0.5 mg α- or β-subunit were brought to 0.4 mL in 6 *M* guanidine hydrochloride, 0.05 *M* Tris-HCl, 0.5 m*M* disodium-EDTA, 65 m*M* dithiothreitol, pH 7.5. Tubes were sealed under N_2, and shaken overnight. Iodoacetic acid was added (fivefold excess over dithiothreitol concentration), and the samples were shaken for 3 h. Reduced and S-carboxymethylated (RCM) samples were dialyzed overnight (6000–8000 Dalton exclusion-limit membrane) against 0.1 *M* NH_4HCO_3 at 4°C and lyophilized.

Enzymatic Release of Asparagine-Linked Oligosaccharide from RCM Peptides

RCM α- and β-subunits were reconstituted (2.5 mg/mL) in 0.3 *M* sodium phosphate, 0.15% SDS, 0.04% NaN_3, pH 7.8. A 50-μL aliquot was denatured at 100°C for 5 min. After cooling, 40 μL were removed and brought to 1% Nonidet P-40/Triton X-100. Five units of PNGase F (Genzyme, Boston, MA) and 60 μL of water were added (final volume = 120 μL), and samples were sealed under N_2. RCM CR129 β-subunit was incubated for 24 h at 37°C with 5 U of PNGase F. A second aliquot of PNGase F was added, and incubation continued 24 h (48 h total). Removal of N-glycans was monitored using reducing SDS-PAGE (16%) (Fig. 3). RCM β-subunit migrated at M_r = 36,000 at 0 h, and M_r = 29,000 after 24- and 48-h incubations, indicating complete removal of N-linked oligosaccharides after one incubation with enzyme. RCM CR129 α-subunit was incubated for three serial 24-h periods (72 h total) with additions of 5 U enzyme each. RCM α-subunit migrated at M_r = 25,000 at 0 h, as three bands (M_r = 25,000, 22,000, and 18,000) after 24 and 48 h, and as one band (M_r = 18,000) after 72 h. This indicated partial removal of one or two oligosaccharides after 24 and 48 h, and complete release in 72 h. One 24-h incubation with 5 U PNGase F was adopted for RCM β-subunit samples and three 24-h incubations with 5 U enzyme each for RCM α-subunit preparations.

Isolation of N-Glycans and Enzymatic Release of Sialic Acid

N-glycans, released by PNGase F, were separated from peptides (RCM α-subunits) and peptides with O-linked oligosaccharides (RCM β-subunits) by ethanol precipitation:

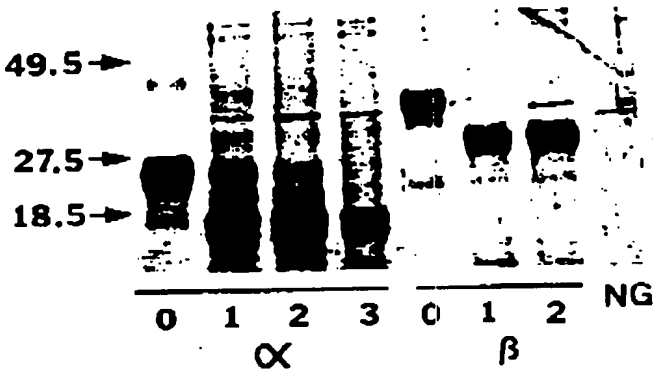

Fig. 3. SDS-PAGE of RCM subunits of CR129 hCG, prior to and following PNGase F digestion. Lanes α0–3 are RCM hCG α-subunit after 0, 1, 2, and 3 d of incubation with PNGase F (enzyme aliquots added at days 0, 1, and 2); lanes β0–2 are RCM hCG β-subunit after 0, 1, and 2 d incubation with PNGase F (enzyme aliquots added at days 0 and 1). NG is the PNGase F control. Migration of molecular weight standards is illustrated by arrows (→).

samples were brought to 1:6.5 (v/v) with 95% ethanol and centrifuged at 145*g* overnight at 4°C. Sample supernatants containing the *N*-glycans were removed, dried, and reconstituted in 0.1 *M* sodium phosphate, pH 5.1, with 0.1% NaN_3. To ensure the complete desialylation of the *N*-glycans with the potential to contain tri- and tetrasialylated oligosaccharides, a lyophilized, tetrasialylated, tetra-antennary oligosaccharide standard (corresponding to tetrasialylated GGGG; Oxford Glycosystems, New York, NY) was reconstituted in sodium phosphate, SDS, NaN_3, Nonidet P-40, and Triton X-100 (as the lyophilized RCM subunits, above), ethanol-precipitated, and the resultant supernatant used as a control to monitor the release of sialic acid. The standard's supernatant was dried and reconstituted in 0.1 *M* sodium phosphate, pH 5.1, with 0.1% NaN_3, and Neuraminidase *Clostridium perfringens* was added at 1.25 U/mL (substrate concentration = 10 μ*M*). The control was incubated for 120 h at 37°C (conditions found necessary owing to the presence of SDS carried forward with the supernatant after ethanol precipitation), and timed aliquots were removed and monitored. Quantitative removal of sialic acid was demonstrated using the chromatography procedures described below.

Resolution and Characterization of Desialylated N-*Glycans*

Desialylated *N*-glycans were injected onto a Dionex HPLC carbohydrate detection system (Sunnyvale, CA), composed of a CarboPac 1 column coupled with a gradient HPLC pump. Glycans were visualized with a Dionex PAD, and the resulting output data were plotted and integrated using a SpectroPhysics Chromjet Integrator (San Jose, CA). The column was eluted at 1 mL/min with NaOH using the oligosaccharide protocol: 9 m*M* for 40 min, 90 m*M* for 15 min, 150–270 m*M* over 35 min, and 270 m*M* for 10 min. The column effluent was continuously mixed via a mixing tee with a postcolumn addition of 225 m*M* NaOH, at 1 mL/min by a Kratos Spectroflow 400 HPLC pump (Ramsey, NJ). Desialylated *N*-glycans and free sialic acid were quantitated by integration of sample peak areas and comparison with oligosaccharide and sialic acid standards *(see below)* (Fig. 4). As confirmation that the oligosaccharide standards and sample peaks were identical in carbohydrate content, individual sample peaks of common elution positions were collected from the CarboPac 1 column, hydrolyzed, and analyzed for carbohydrate composition; subsequently, the oligosaccharide contents of the RCM α- and β-subunits was determined by comparison of the PNGase F-released glycans with the elution of the oligosaccharide standards (Fig. 4). For peak collection, high-pH column effluent was directed from the CarboPac 1 column into a micromembrane suppressor vs 70 m*N* H_2SO_4 (Dionex Anion Micromembrane Suppressor AMMS-1), rendering the column effluent pH-neutral. Collected peaks were dried and hydrolyzed according to a modification of the method of Hardy et al. *(48)*, at 3.2 *N* trifluoroacetic acid (TFA), under N_2, for 4 h at 100°C. Hydrolysates were dried, reconstituted with water, and injected onto a CarboPac 1 column using the monosaccharide protocol. The column was eluted at 0.4 mL/min with NaOH: 18.5 m*M* for 30 min followed by 9.25 m*M* for 13 min. Column effluent was continuously mixed with a postcolumn addition of 300 m*M* NaOH at 1 mL/min. The monosaccharide composition was calculated by integration of hydrolysate peak areas and comparison with known amounts of monosaccharide standards (Sigma, St. Louis, MO) (Fig. 5).

N-*Glycan Standards*

N-glycan standards (Oxford Glycosystems and Dionex Corp.) included biantennary oligosaccharides with each antenna terminating at galactose (GG), triantennary oligosaccharides terminating at galactose (GGG), and the same two with fucose α1,6-linked to the proximal *N*-acetylglucosamine (GGF and GGGF). Also included was a tetraantennary oligosaccharide terminating at galactose (GGGG) and *N*-glycans with antennae terminating at *N*-acetylglucosamine (AAF, AA, AAA, AAAA) or terminating at mannose (MM and MMF) (Fig. 4).

Two sample peaks were shown to be carbohydrate in nature by monosaccharide compositional analysis, but did not coelute with the listed *N*-glycan standards. Their monosaccharide ratios were determined and their molecular weights were analyzed by matrix-assisted laser desorption ionization (MALDI) mass spectrometry (Fison Instruments, Manchester, UK) at The Keck Foundation Biotechnology Resource Facility at Yale University. Monosaccharide compositional analysis revealed a structure with a Man:GlcNAc:Gal ratio of 3:3:1. The observed mass/charge *(m/z)* was 1299.8 corresponding to the (mass

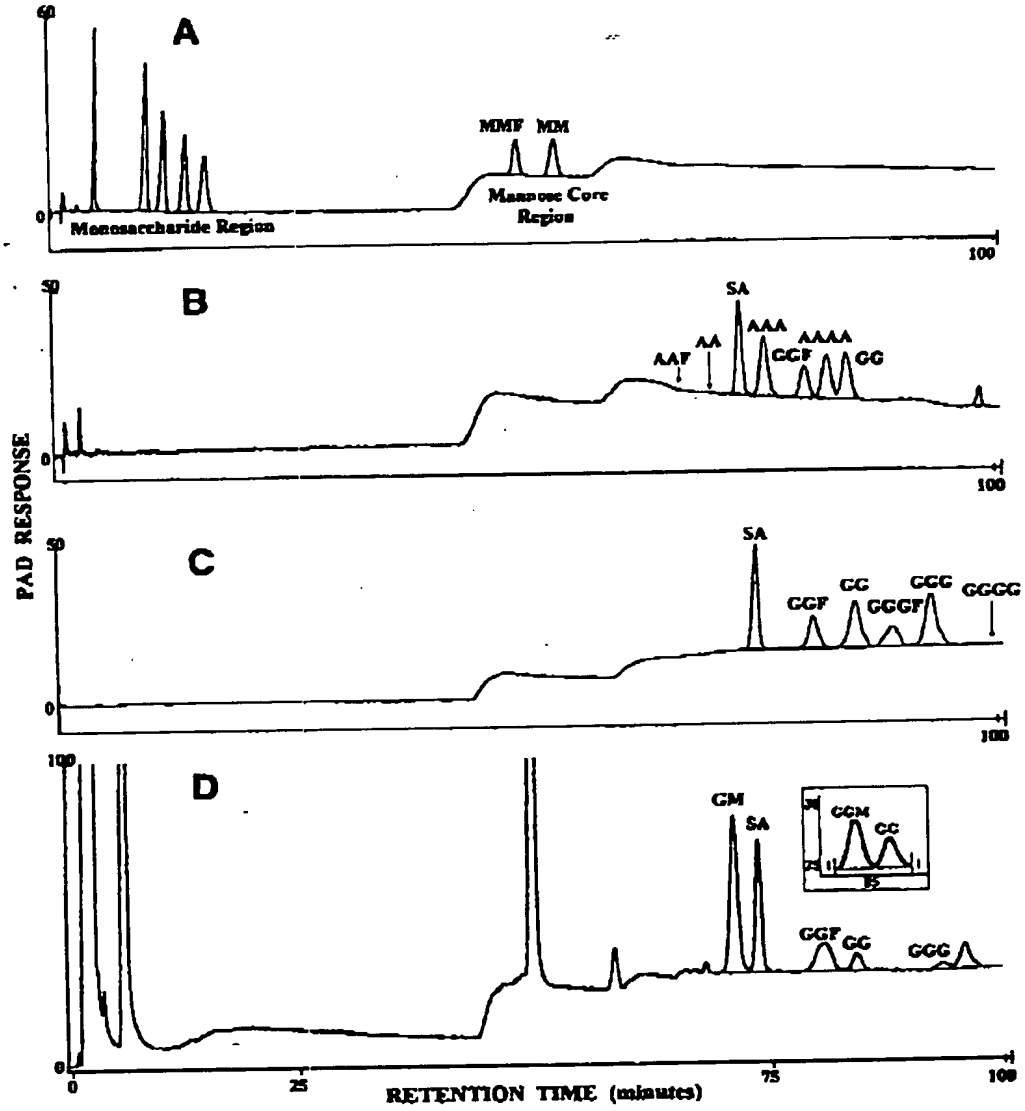

Fig. 4. Separation of intact and truncated bi-, tri- and tetra-antennary N-linked oligosaccharide and sialic acid standards on a high-pH ion-exchange HPLC column using the oligosaccharide protocol described in Materials and Methods. (A) Elution profile of a mixture of 625 pmol standard monosaccharides (Fuc, $GalNH_2$, $GlcNH_2$, Gal, and Man) and 200 pmol oligosaccharide standards MMF and MM. (B) Elution profile of a mixture of 825 pmol sialic acid standard and 200 pmol oligosaccharide standards: AAA, GGF, AAAA, and GG. (C) Elution profile of a mixture of 825 pmol sialic acid standard and 210 pmol oligosaccharide standards: GGF, GG, GGGF, and GGG. (D) Elution profile of desialylated N-glycans and neuraminidase-released sialic acid from choriocarcinoma C5 α-subunit. Insert: Excerpt from the elution profile of N-glycans from diabetic D1 α-subunit illustrating the separation of GGM and GG using the modified oligosaccharide protocol described in Materials and Methods. The PAD was set at 300 nA full scale. PAD response is in relative units.

+ sodium)$^+$ ion and consistent with the monosaccharide composition. A carbohydrate structure of this molecular weight and composition has been identified previously in hCG *(19,21)*. The sequence is: Galβ1→4GlcNAcβ1→2Manα1→3(Manα1→6)Manβ1→4GlcNAcβ1→4GlcNAc; this monoantennary structure was designated GM (Fig. 6).

The second peak that did not coelute with a known standard eluted closely with GG in the oligosaccharide protocol. Complete separation was achieved with a modified NaOH protocol: addition of a 150-m*M* step for 10 min prior to the 150–270 m*M* gradient. The extended oligosaccharide protocol completely resolves these peaks, with the later-eluting peak eluting in the position of the GG standard. Both peaks were neutralized and individually collected via the in-line micromembrane suppressor described above, and their monosaccharide compositions and

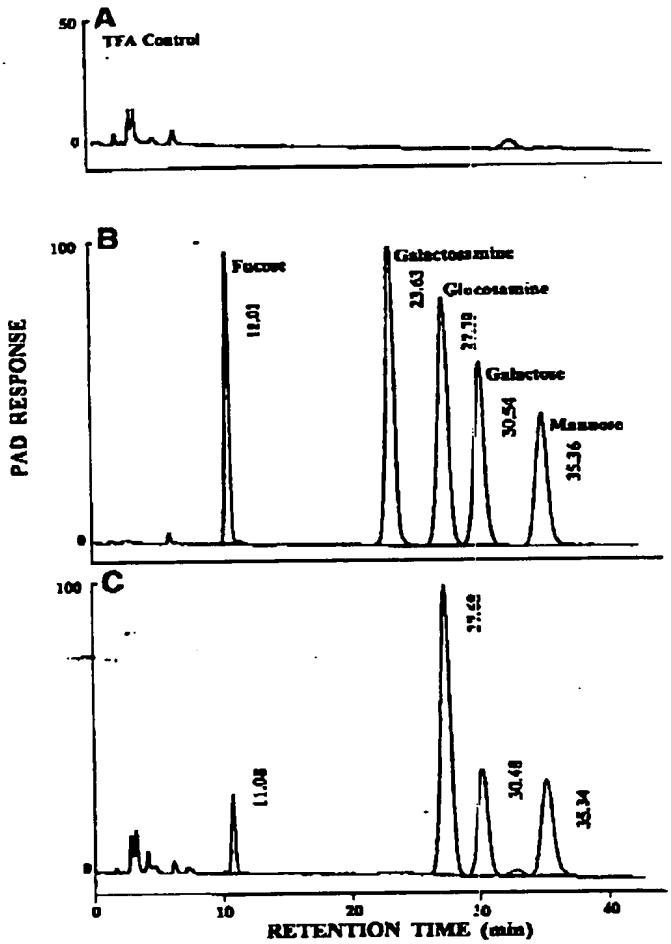

Fig. 5. Separation of monosaccharide standards on a high-pH ion-exchange HPLC column using the monosaccharide protocol. (A) Elution profile of a TFA control hydrolysate. (B) Elution profile of a 625-pmol mixture of standard monosaccharides. (C) Elution profile of a representative oligosaccharide hydrolysate showing that of fucosylated biantennary GGF. Comparison of integrated peak areas of oligosaccharide hydrolysate with those of known amounts of monosaccharide standards (Panel B) yielded a monosaccharide composition of 1.0 (1.0) Fuc, 4.12 (4.0) GlcNAc (measured as $GlcNH_2$), 2.1 (2.0) Gal, and 2.82 (3.0) Man. The PAD was set at 100 nA full scale. PAD response is in relative units.

molecular weights determined. Both peaks contained the same monosaccharide composition: Man, GlcNAc, and Gal in the ratio 3:4:2. The observed molecular weight of a GG standard control was *m/z* = to 1664.72 corresponding to the (mass + sodium)$^+$ ion. The observed molecular weights of the two sample peaks were 1664.83 and 1664.74, corresponding to the (mass + sodium)$^+$ ion and consistent with the monosaccharide composition. GG and a second biantennary oligosaccharide with the same monosaccharide composition have been reported previously *(25,26)*. The second peak has two *N*-acetyllactosamine antennae attached at the C-2 and C-4 positions of the same α-mannosyl residue of the trimannosyl core: Galβ1→4GlcNAcβ1→2(Galβ1→4GlcNAcβ1→4)Manα1→3(Manα1→6)Manβ1→4GlcNAcβ1→4GlcNAc. This structure, designated GGM, although containing the same monosaccharide composition as GG, has a terminal mannose or an additional nonreducing terminus (Fig. 6).

Isolation, Resolution, and Characterization of O-Glycans

Following PNGase F-release of N-linked oligosaccharides, mixtures of *O*-glycopeptides and free *N*-glycans were separated by ethanol precipitation (described above). Precipitates containing the *O*-glycopeptides were reconstituted in water and injected onto a 4 × 250 mm Vydac C_4 reverse-phase column using a Kratos Spectroflow HPLC system equipped with a model 430 Gradient Former and a model 400 pump. The column was eluted at 0.8 mL/min in 0.1% TFA with a 0–60% acetonitrile linear gradient over 90 min. Peaks containing *O*-glycopeptides were visualized at 210 nm with an Applied Biosystems 783 Programmable Absorbance Detector, collected directly into vials for subsequent hydrolyses, and immediately dried.

This laboratory and others have previously shown that there are two *O*-glycan core structures on the β-subunit of hCG: Galβ1→3GalNAc*(22,23)*andGalβ1→4GlcNAcβ1→6(Galβ1→3)GalNAc*(23,24)* (Fig. 6). The presence of GlcNAc and a 2:1 ratio of Gal distinguish the tetra- from the disaccharide structure. Compositional analysis was used to quantitate monosaccharides and to determine the ratio of tetrasaccharide to disaccharide structures. Purified *O*-glycopeptides were hydrolyzed according to a modification of the method of Hardy et al. *(48)*, at 3 *N* HCl for 140 min at 100°C, under N_2, and then dried. The hydrolysates were reconstituted with water, injected onto a CarboPac 1 column, eluted with the monosaccharide protocol, and monosaccharide composition determined as described above. To determine the sialic acid content, *O*-glycopeptides were hydrolyzed using a modification of the method of Blithe: 0.1 *M* TFA at 80°C for 50 min *(31)*. Hydrolysates were dried, reconstituted with water, and injected onto the CarboPac 1 column using the oligosaccharide gradient protocol, and sialic acid content determined as described above.

Amino-Terminal Sequence Analysis

Amino-terminal sequence analysis was performed by The W. M. Keck Foundation Biotechnology Resource Facility using an Applied Biosystems model 470A gas-phase sequencer equipped with an on-line HPLC system for identification of phenylthiohydantoin amino acids. Peaks were quantitated with Nelson Analytical Xtrachrome software (South Plainfield, NJ) using standard procedures.

Carboxypeptidase Y Analysis

Carboxyl-terminal sequences were determined for nicked β-subunit preparations M4, C2, and C5 using carboxypepti-

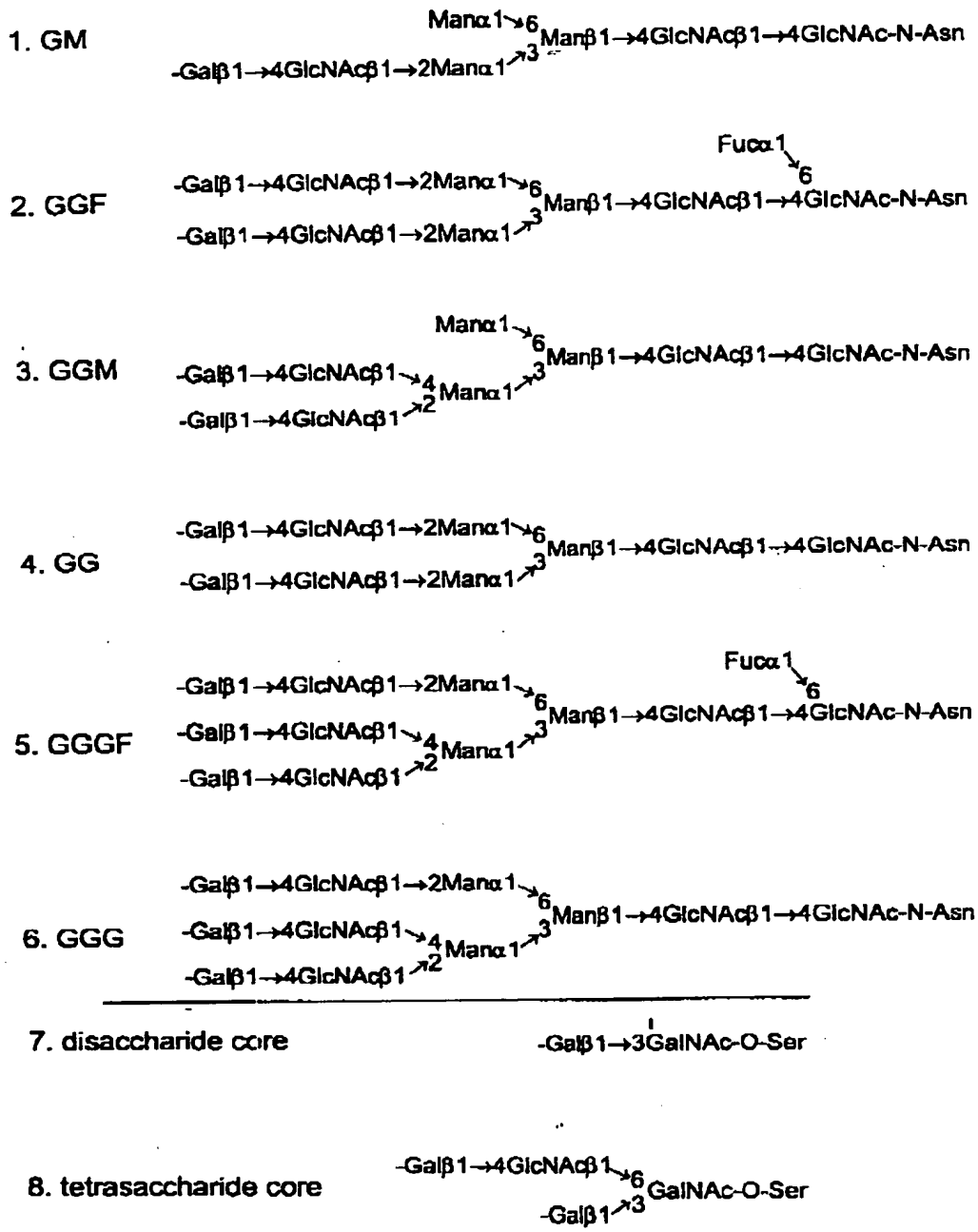

Fig. 6. Structures of the asialo N- and O-linked oligosaccharides. Structures 1–6 are the asparagine-linked oligosaccharides in the order of elution from the high-pH ion-exchange HPLC column (Fig. 4). Structures 7 and 8 are the serine-linked di- and tetrasaccharide core structures. Hyphens (–) on Gal and GalNAc residues indicate potential attachment sites of sialic acid.

dase Y digestion followed by amino acid composition analysis. Samples were dissolved in 25 µL 0.1 *M* sodium acetate, pH 5.5, containing 8 *M* urea and denatured by incubation for 10 min at 60°C. After cooling, carboxypeptidase Y (sequencing grade) was added in 25 µL water (enzyme:substrate ratio = 1:15) and mixtures incubated for 90 min at 37°C. Products of samples and controls (nonincubated reaction mixture = time-zero control; incubated reaction mixture minus substrate = substrate control) were dried and given to The W. M. Keck Foundation Biotechnology Resource Facility for amino acid composition analysis.

Acknowledgments

The authors wish to thank K. Stone and K. Williams of The W. M. Keck Foundation Biotechnology Resource Facility at Yale University for amino-terminal sequencing

of α- and β-subunits. The authors also wish to thank S. Birken for the gift of reference standards CR127 hCG and for CR129 α- and β-subunits and J. C. Morris for the gift of purified choriocarcinoma C7 hCG. Additionally, the authors are appreciative of the donation of urine samples acquired by K. Bagshawe, J. Belinson, E. Kohorn, M. Ozturk, S. Rotmensch, E. Shapiro, K. Yazaki, and W. Yixun. For gifts of FBT11, H7, and 2119-12 antibodies, the authors also wish to thank J.-M. Bidart of the Institut Gustave Roussy (Villejuif Cedex, FR), R. O. Hussa and M. Story while at the Medical College of Wisconsin, and K. May of Unipath, Ltd. (Bedford, UK). This work was supported by NIH grants CA-44131 (to L. A. C.) and HD-15454 (to J. W. L.).

References

1. Roche, P. C. and Ryan, R. J. (1985). In: *Luteinizing Hormone Action and Receptors*. Ascoli, M. (ed.). CRC: Boca Raton, pp. 17–56.
2. Hunzicker-Dunn, M. H. and Birnbaumer, L. (1985). In: *Luteinizing Hormone Action and Receptors*. Ascoli, M. (ed.). CRC: Boca Raton, pp. 57–134.
3. Harbour-McMenamin, D., Smith, E. M., and Blalock, J. E. (1986). *Proc. Natl. Acad. Sci. USA* 83, 6834–6838.
4. Yagel, S., Geva, T. E., Solomon, H., Shimonovitz, S., Reich, R., Finci-Yeheskel, Z., Mayer, M., and Milwidsky, A. (1993). *J. Clin. Endocrinol. Metab.* 77, 1506–1511.
5. Pierce, J. G. and Parsons, T. F. (1981). *Ann. Rev. Biochem.* 50, 465–495.
6. Wu, H., Lustbader, J. W., Liu, Y., Canfield, R. E., and Hendrickson, W. A. (1994). *Structure* 2, 545–558.
7. Li, E., Tabas, I., and Kornfeld, S. (1978). *J. Biol. Chem.* 253, 7762–7770.
8. Peters, B. P., Krzesicki, R. F., Hartle, R. J., Perini, F., and Ruddon, R. W. (1984). *J. Biol. Chem.* 259, 15,123–15,130.
9. Kornfeld, S., Li, E., and Tabas, I. (1978). *J. Biol. Chem.* 253, 7771–7778.
10. Birken, S. and Canfield, R. E. (1977). *J. Biol. Chem.* 252, 5386–5392.
11. Keutmann, H. T. and Williams, R. M. (1977). *J. Biol. Chem.* 252, 5393–5397.
12. Huth, J. R., Mountjoy, K., Perini, F., and Ruddon, R. W. (1992). *J. Biol. Chem.* 267, 8870–8879.
13. Birken, S. and Canfield, R. E. (1978). In: *Structure and Function of the Gonadotropins*. McKerns, K. W. (ed.). Plenum: New York, pp. 47–80.
14. Kardana, A., Elliott, M. M., Gawinowicz, M.-A., Birken, S., and Cole, L. A. (1991). *Endocrinology* 129, 1541–1550.
15. Bidart, J.-M., Puisieux, A., Troalen, F., Foglietti, M. J., Bohuon, C., and Bellet, D. (1988). *Biochem. Biophys. Res. Commun.* 154, 626–632.
16. Nishimura, R., Ide, K., Utsunomiya, T., Kitajima, T., Yuki, Y., and Mochizuki, M. (1988). *Endocrinology* 123, 420–425.
17. Cole, L. A., Kardana, A., and Birken, S. (1989). *Serono Symposium* 65, 59–78.
18. Kessler, M. J., Reddy, M. S., Shah, R. H., and Bahl, O. P. (1979). *J. Biol. Chem.* 254, 7901–7908.
19. Endo, Y., Yamashita, K., Tachibana, Y., Tojo, S., and Kobata, A. (1979). *J. Biochem. (Tokyo)* 85, 669–679.
20. Nilsson, B., Rosen, S. W., Weintraub, B. D., and Zopf, D. A. (1986). *Endocrinology* 119, 2737–2743.
21. Weisshaar, G., Hiyama, J., and Renwick, A. G. C. (1991). *Glycobiology* 1, 393–404.
22. Kessler, M. J., Mise, T., Ghai, R. D., and Bahl, O. P. (1979). *J. Biol. Chem.* 254, 7909–7914.
23. Cole, L. A. (1987). *J. Clin. Endocrinol. Metab.* 65, 811–813.
24. Amano, J., Nishimura, R., Mochizuki, M., and Kobata, A. (1988). *J. Biol. Chem.* 263, 1157–1165.
25. Mizuochi, T., Nishimura, R., Derappe, C., Taniguchi, T., Hamamoto, T., Mochizuki, M., and Kobata, A. (1983). *J. Biol. Chem.* 258, 14,126–14,129.
26. Mizuochi, T., Nishimura, R., Taniguchi, T., Utsunomiya, T., Mochizuki, M., Derappe, C., and Kobata, A. (1985). *Jpn. J. Cancer Res. (Gann)* 76, 752–759.
27. Skarulis, M. C., Wehmann, R. E., Nisula, B. C., and Blithe, D. L. (1992). *J. Clin. Endocrinol. Metab.* 75, 91–96.
28. Wide, L., Lee, J.-Y., and Rasmussen, C. (1994). *J. Clin. Endocrinol. Metab.* 78, 1419–1423.
29. Diaz-Cueto, L., Mendez, J. P., Burrios-de-Tomasi, J., Lee, J.-Y., Wide, L., Veldhuis, J. D., and Ulloa-Aguirre, A. (1994). *J. Clin. Endocrinol. Metab.* 78, 890–897.
30. Stockell Hartree, A. and Renwick, A. G. C. (1992). *Biochem. J.* 287, 665–679.
31. Blithe, D. L. (1990). *Endocrinology* 216, 2788–2799.
32. Williams, D., Longmore, G., Matta, K. L., and Schachter, H. (1980). *J. Biol. Chem.* 255, 11,253–11,261.
33. Birken, S., Chen, Y., Gawinowicz, M.-A., Lustbader, J. W., Pollack, S., Agosto, G., Buck, R., and O'Connor, J. (1993). *Endocrinology* 133, 1390–1397.
34. Yamashita, K., Totani, K., Iwaki, Y., Takamisawa, I., Tateishi, N., Higashi, T., Sakamoto, Y., and Kobata, A. (1989). *J. Biochem. (Tokyo)* 105, 728–735.
35. Lustbader, J., Birken, S., Pollack, S., Levinson, L., Bernstine, E., Hsiung, N., and Canfield, R. (1987). *J. Biol. Chem.* 262, 14,204–14,212.
36. Calvo, F. O. and Ryan, R. J. (1985). *Biochemistry* 24, 1953–1959.
37. Matzuk, M. M., Keene, J. L., and Boime, I. (1989). *J. Biol. Chem.* 264, 2409–2414.
38. Gordon, W. L. and Ward, D. N. (1985). In: *Luteinizing Hormone Action and Receptors*. Ascoli, M. (ed.). CRC: Boca Raton, pp. 174–197.
39. Ryan, R. J., Charlesworth, M. C., McCormick, D. J., Milius, R. P., and Keutmann, H. T. (1988). *FASEB J.* 2, 2661–2669.
40. Keutmann, H. T., Ratanabanagkoon, K., Pierce, M. W., Kitzmann, K., and Ryan, R. J. (1983). *J. Biol. Chem.* 258, 14,521–14,526.
41. Sakakibara, R., Miyazaki, S., and Ishiguro, M. (1990). *J. Biochem.* 107, 858–862.
42. Cole, L. A., Kardana, A., Andrade-Gordon, P., Gawinowicz, M.-A., Morris, J. C., Bergert, E. R., O'Conner, J., and Birken, S. (1991). *Endocrinology* 129, 1559–1567.
43. Matzuk, M. M., Krieger, M., Corless, C. L., and Boime, I. (1987). *Proc. Natl. Acad. Sci. USA* 84, 6354–6358.
44. LaPolt, P. S., Nishimori, K., Fares, F. A., Perlas, E., Boime, I., and Hsueh, A. J. (1992). *Endocrinology* 131, 2514–2520.
45. Huang, J., Chen, F., and Puett, D. (1993). *J. Biol. Chem.* 268, 9311–9315.
46. Kardana, A. and Cole, L. A. (1992). *Clin. Chem.* 38, 26–33.
47. Elegbe, R. A., Pattillo, R. A., Hussa, R. O., Hoffmann, R. G., Damole, I. O., and Finlayson, W. E. (1984). *Obstet. Gynecol.* 63, 335–337.
48. Hardy, M. R., Townsend, R. R., and Lee, Y. C. (1988). *Anal. Biochem.* 170, 54–62.
49. Morgan, F. J., Birken, S., and Canfield, R. E. (1975). *J. Biol. Chem.* 250, 5247–5258.